

Analysis of reflectometric measurements losses of spliced single mode telecommunication fibers with significantly different parameters

MAREK RATUSZEK

Institute of Telecommunication, University of Technology and Agriculture, Kaliskiego 7,
85-796 Bydgoszcz, Poland

In this paper there have been presented theoretical and basing on experiments analysis of one-way and two-way reflectometric measurements of spliced single mode telecommunication fibers with different refractive index profiles, received in various combinations of joints. In the analysis the dependence of one-way and two-way reflectometric measurements of splice loss on the mode field radii quotient and on the shift of axes of the spliced fibers as a function of measurement wavelength has been taken into account. On the basis of one-way reflectometric measurements a method explicitly proving the existence of a transient area in the spliced fibers has been presented.

Keywords: reflectometry, fibers.

1. Introduction – losses of connected fibers

The splice (connection) loss is computed in terms of the fraction of incident power that is coupled from the incident fundamental mode of fiber 1 to the fundamental mode of fiber 2 – Fig. 1. The power coupling efficiency between two fibers weakly guiding (telecommunication fibers) is given by [1, 2]:

$$\eta = \frac{4\beta_1\beta_2}{(\beta_1 + \beta_2)^2} \frac{\left| \int_{-\infty}^{\infty} \int_{-\infty}^{\infty} E_1(x, y) E_2^*(x, y) dx dy \right|^2}{\int_{-\infty}^{\infty} \int_{-\infty}^{\infty} E_2(x, y) E_2^*(x, y) dx dy \int_{-\infty}^{\infty} \int_{-\infty}^{\infty} E_1(x, y) E_1^*(x, y) dx dy} \quad (1)$$

where: $E_1(x, y)$ and $E_2(x, y)$ are transverse components of the modal electric field of the fiber 1 and 2, respectively (see Fig. 1), β_1 and β_2 are propagation constants of the fiber 1 and 2, respectively, * – denote conjugate function.

For optical fibers with circular symmetry (telecommunication fibers) Eq. (1) may be transformed to cylindrical co-ordinates:

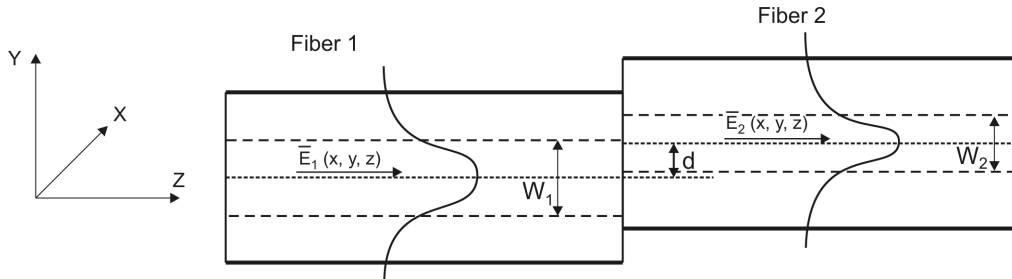


Fig. 1. Fibers connection with axes shift d .

$$\eta = \frac{4\beta_1\beta_2}{(\beta_1 + \beta_2)^2} \frac{\left| \int_0^\infty \left(\int_0^{2\pi} E_1 E_2^* r d\varphi \right) dr \right|^2}{\int_0^\infty \left(\int_0^{2\pi} E_2 E_2^* r d\varphi \right) dr \int_0^\infty \left(\int_0^{2\pi} E_1 E_1^* r d\varphi \right) dr}. \quad (2)$$

When two single mode telecommunication fibers with circular symmetry and weakly guiding are connected co-axially, then $\beta_1 \approx \beta_2$ and the transverse components of the modal electric field are usually well approximated by Gaussian function [1–3]:

$$E(x, y) = \exp\left[-\frac{1}{2}\left(\frac{r}{W}\right)^2\right] \quad (3)$$

where: W – mode field radius, $r = \left(x^2 + y^2\right)^{\frac{1}{2}}$ – distance from the center of the fiber.

Substituting Eq. (3) into Eq. (2), we obtain:

$$\eta = \frac{16\beta_1\beta_2}{(\beta_1 + \beta_2)^2} \frac{W_1^2 W_2^2}{(W_1^2 + W_2^2)^2}. \quad (4)$$

In weak guiding regime $\beta_1 \approx \beta_2$ and we obtain:

$$\eta = 4 \frac{W_1^2 W_2^2}{(W_1^2 + W_2^2)^2}. \quad (5)$$

When the same fibers are not concentric, with axis shifted by value d (Fig. 1) then [1]:

$$E(x, y) = \exp\left[-\frac{1}{2} \frac{(x+d)^2 + y^2}{W^2}\right] \quad (6)$$

and we obtain [1, 4]:

$$\eta = 4 \frac{W_1^2 W_2^2}{(W_1^2 + W_2^2)^2} \exp\left(-\frac{d^2}{W_1^2 + W_2^2}\right). \quad (7)$$

2. Reflectometric measurements losses of connected fibers

According to [5] the backscattered power detected by OTDR (optical time domain reflectometer) from a point immediately preceding the splice is given by (the subscript 1 refers to the input fiber):

$$P_1 = P_0 S_1 \exp(-2\alpha_1 L_1) \quad (8)$$

where: P_0 – the initial power level [dBm], L – the fiber length [km], α – the attenuation coefficient [1/km], S – the backscatter coefficient, the latter being given by [6]:

$$S = \frac{\frac{3}{2} (\text{NA})^2}{\left(\frac{W}{a}\right)^2 V^2 n^2} \quad (9)$$

where: NA – the numerical aperture, W – the mode field radius, a – the core radius, V – normalized frequency, n – the core refractive index at the core radius.

The normalized frequency of the fiber is defined as usual [1–3, 7]:

$$V = kan\sqrt{2\Delta} = ka\text{NA} \quad (10)$$

where: $k = 2\pi/\lambda$ (λ – the wavelength), $\Delta = (n^2 - n_{\text{clad}}^2)/2n^2$.

Substituting Eq. (10) into Eq. (9) we obtain (the subscript 1 refers to the input fiber) [8]:

$$S_1 = 0.038 \left(\frac{\lambda}{n_1 W_1}\right)^2. \quad (11)$$

The backscattered power detected by OTDR from a point immediately following the splice is given by [5]:

$$P_2 = P_0 S_1 \eta_{12} \eta_{21} \exp(-2\alpha_1 L_1) \quad (12)$$

where: η_{12} – the power coupling efficiency from the fiber 1 to the fiber 2, η_{21} – the corresponding quantity in the reverse direction and $\eta_{12} = \eta_{21} = \eta$ – see Eqs. (5) and (7), S_2 – the backscatter coefficient of the fiber behind the splice is given by:

$$S_2 = 0.038 \left(\frac{\lambda}{n_2 W_2} \right)^2. \quad (13)$$

One-way A_{12} fiber loss from 1→2 is:

$$2A_{12} = -10 \log \frac{P_2}{P_1}. \quad (14)$$

Thus, applying (8), (12) and (7) we obtain:

$$\frac{P_2}{P_1} = \left(\frac{n_1 W_1}{n_2 W_2} \right)^2 \eta_{12} \eta_{21}, \quad (15)$$

$$\begin{aligned} 2A_{12} &= -10 \log \frac{P_2}{P_1} = \\ &= 20 \log \frac{n_2}{n_1} + 20 \log \frac{W_2}{W_1} + 40 \log \left[\frac{1}{2} \left(\frac{W_1}{W_2} + \frac{W_2}{W_1} \right) \right] + 20 \log \left[\exp \left(\frac{d^2}{W_1^2 + W_2^2} \right) \right]. \end{aligned} \quad (16)$$

Hence, one-way apparent splice loss in the direction 1→2 is:

$$A_{12} = 10 \log \frac{n_2}{n_1} + 10 \log \frac{W_2}{W_1} + 20 \log \left[\frac{1}{2} \left(\frac{W_1}{W_2} + \frac{W_2}{W_1} \right) \right] + 4.34 \left(\frac{d^2}{W_1^2 + W_2^2} \right). \quad (17)$$

And similarly one-way apparent splice loss from 2→1 is:

$$A_{21} = 10 \log \frac{n_1}{n_2} + 10 \log \frac{W_1}{W_2} + 20 \log \left[\frac{1}{2} \left(\frac{W_1}{W_2} + \frac{W_2}{W_1} \right) \right] + 4.34 \left(\frac{d^2}{W_1^2 + W_2^2} \right). \quad (18)$$

Real splice loss is an arithmetic mean of (17) and (18) including signs A_{12} and A_{21} :

$$A_S = \frac{A_{12} + A_{21}}{2} = 20 \log \left[\frac{1}{2} \left(\frac{W_1}{W_2} + \frac{W_2}{W_1} \right) \right] + 4.34 \left(\frac{d^2}{W_1^2 + W_2^2} \right). \quad (19)$$

3. Reflectometric measurements analysis

Reflectometric measurements of optical losses are considered to be less precise than transmission measurements. However, the analysis of reflectometric measurements of losses, that is splices loss of fibers, provides a lot of information which cannot be achieved from transmission measurement analysis. It results from the principle of reflectometric analysis based on backscattered power. One-way splice loss contains information about true splice loss and about the types of spliced fibers. It is important because in fiber tracks measurement practice we often do not know what type of fibers we join.

Expressions (17) and (18) describe one-way splice loss values. The first and second components in the expressions (17) and (18) result from the measurement rule (backscattered power), and can assume positive and negative values for splicing fibers of different n and W . The third and fourth components in the Eqs. (17) and (18) express optical coupling between the spliced fibers, and they are always positive.

With the assumptions of concentric splicing of fibers of different types, that is for $d = 0$ and $W_1 \neq W_2$ and $n_1 \neq n_2$, one of the reflectometric measurements is always negative since if $W_1 \neq W_2$ and, *e.g.*, $W_1 > W_2$ and $n_1 \neq n_2$ and, *e.g.*, $n_1 > n_2$ one gets:

– a case of always positive $A_{21}^{(+)}$

$$10 \log \frac{W_1}{W_2} > 20 \log \left[\frac{1}{2} \left(\frac{W_1}{W_2} + \frac{W_2}{W_1} \right) \right]; \quad (20)$$

– a case of always negative $A_{12}^{(-)}$

$$\left| 10 \log \frac{W_2}{W_1} \right| > 20 \log \left[\frac{1}{2} \left(\frac{W_1}{W_2} + \frac{W_2}{W_1} \right) \right]. \quad (21)$$

The values of components $10 \log(n_1/n_2)$ – positive and $10 \log(n_2/n_1)$ – negative, although they additionally increase the positive value A_{21} and the negative value A_{12} , respectively, can be neglected. For example, while splicing the fibers with significantly different numerical apertures: $NA_1 = 0.16$ (dispersion shifted SMF), and $NA_2 = 0.12$ (matched cladding SMF), their refractive indices in the cores (with doping GeO_2) for $\lambda = 1310$ nm – calculated from Sellmaier's principle [4] are respectively $n = 1.4557$ and $n = 1.4515$. Thus, the values of components $10 \log(n_1/n_2) = 0.0125$ dB and

$10\log(n_2/n_1) = -0.0125$ dB actually do not have influence on one-way loss A_{21} and A_{12} , and they can be neglected in the analysis.

3.1. Dependence of one-way (apparent) and two-way (true) losses of splices of measurement wavelengths

When analyzing the expressions (17), (18) and (19), with the components $10\log(n_1/n_2)$ and $10\log(n_2/n_1)$ neglected, the presented below splicing cases can be distinguished.

Case I. Central splicing, *i.e.*, $d = 0$ and here:

1. $W_1 = W_2$,
2. $W_1 \neq W_2$ and when $W_1 > W_2$ then W_1/W_2 decreases along with the wavelength λ ,
3. $W_1 \neq W_2$ and when $W_1 > W_2$ then W_1/W_2 increases along with the wavelength λ ,
4. $W_1 \neq W_2$ and W_1/W_2 does not change with the wavelength λ .

Case II. Splicing with an axis shift, *i.e.*, $d \neq 0$ and here:

1. $W_1 = W_2$,
2. $W_1 \neq W_2$ and when $W_1 > W_2$ then W_1/W_2 decreases along with the wavelength λ ,
3. $W_1 \neq W_2$ and when $W_1 > W_2$ then W_1/W_2 increases along with the wavelength λ ,
4. $W_1 \neq W_2$ and W_1/W_2 does not change with the wavelength λ .

Suitable types of spliced fibers can be assigned to the above presented cases. Thus, theoretically, cases I.1 and II.1 concern splicing of the same types of fibers. Cases I.2 and II.2 concern splicing of standard fibers (SMF – standard single mode fiber) – step refractive index profile – Fig. 2, with shifted dispersion fibers (DS SMF – dispersion shifted single mode fiber), and with non-zero dispersion fibers (NZDS SMF – non-zero dispersion shifted single mode fiber) with refractive index profile presented in Fig. 2.

In cases I.2 and II.2 the ratio of mode field radii decreases along with the wavelength rise – Fig. 3 [9].

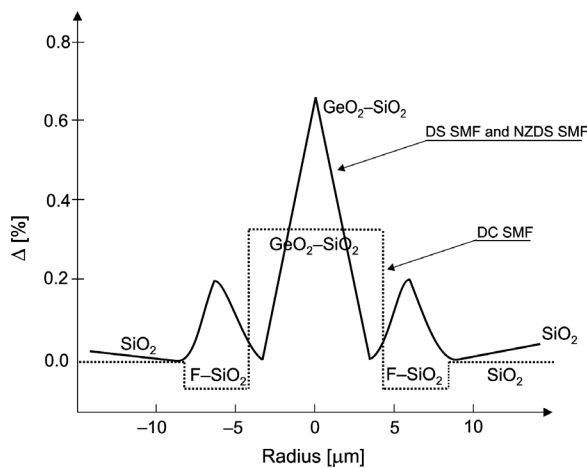


Fig. 2. Refractive index profile in fibers DC SMF (G.652), DS SMF (G.653) and NZDS SMF (G.655) [4, 10].

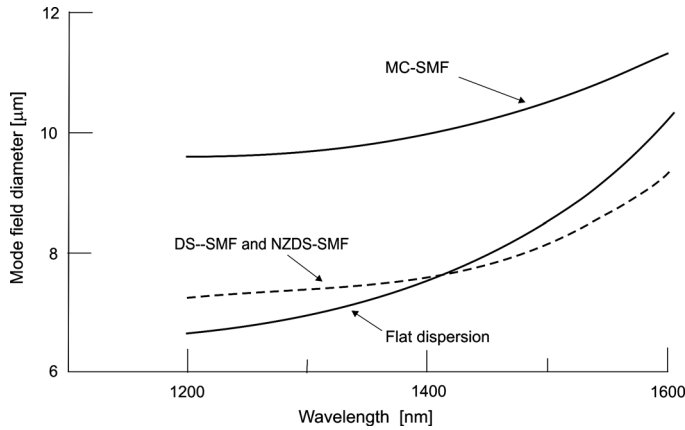


Fig. 3. Dependence of the mode field diameters on wavelengths for fibers SMF, NZDS-SMF(DS SMF) and with flat dispersion characteristics [9].

Cases I.3 and II.3 concern splicing of fibers with step index and W -type refractive index profiles [4], *i.e.*, two types of standard fibers: MC SMF (matched cladding single mode fiber) with DC SMF (depressed cladding single mode fiber), as in this case the mode field radii ratio increases along with the rise of wavelength [10].

Cases I.4 and II.4 concern splicing of fibers of the same type, although differing with their mode field radii within the accepted value of MFD (mode field diameter) distribution.

It should also be noted that along with the wavelength rise, *i.e.*, the mode field increase, the loss resulting only from the lack of concentricity of the joint (case of II.1) decreases and it is of course always positive regardless the measurement direction.

3.2. Reflectometric measurements of spliced fibers of different types – theoretical analysis and test results

3.2.1. Central splicing $d = 0$

Case I.1. – $W_1 = W_2$, $d = 0$. In the expressions (17) and (18) we neglect the first component (insignificant influence) as well as the fourth one ($d = 0$):

$$A_{12} = 10 \log \frac{W_2}{W_1} + 20 \log \left[\frac{1}{2} \left(\frac{W_1}{W_2} + \frac{W_2}{W_1} \right) \right], \quad (22)$$

$$A_{21} = 10 \log \frac{W_1}{W_2} + 20 \log \left[\frac{1}{2} \left(\frac{W_1}{W_2} + \frac{W_2}{W_1} \right) \right]. \quad (23)$$

If $W_1 = W_2$ (from the point of view of losses, splicing of identical fibers) $A_{12} = A_{21} = A_S = 0$ and of course they do not depend on the wavelengths.

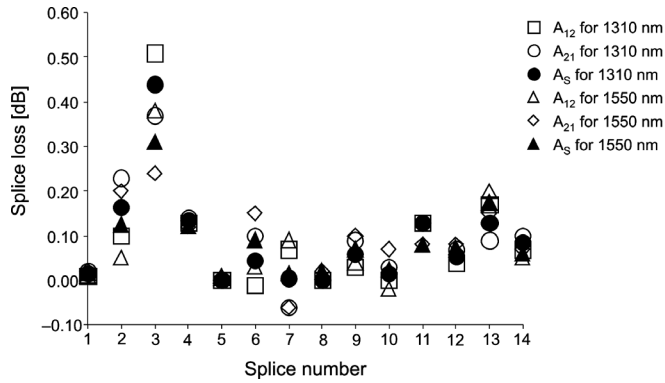


Fig. 4. Loss of 14 splices of joined fibers MC SMF (examples from the used fiber track) for $\lambda = 1310$ nm and $\lambda = 1550$ nm. Reflectometer MW90700B by Anritsu firm was used.

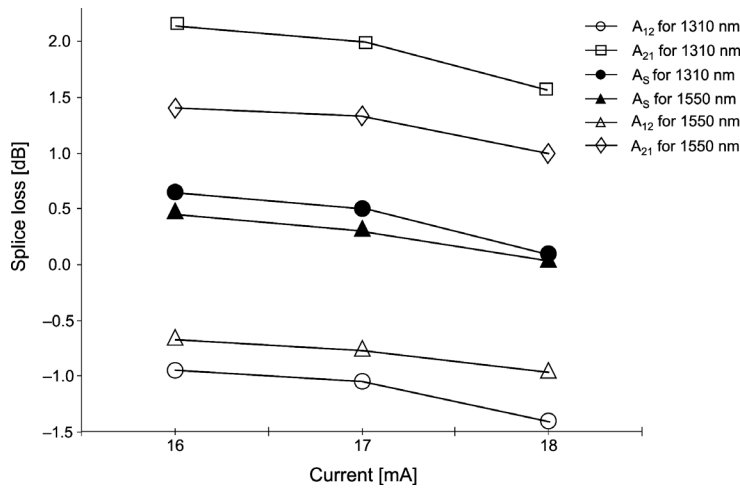


Fig. 5. Dependence of the loss (reflectometric measurement) of splices of fibers MC SMF ($2W_1|_{1310\text{nm}} = 9.3 \pm 0.5 \mu\text{m}$, $2W_1|_{1550\text{nm}} = 10.5 \pm 1 \mu\text{m}$) with NZDS SMF of the true-wave type ($2W_2|_{1310\text{nm}} \approx 6.7 \mu\text{m}$, $2W_2|_{1550\text{nm}} = 8.4 \pm 0.6 \mu\text{m}$) on the splicing current – Ericsson splicer 925RTC. Splicing time $t = 2$ sec.

In practice most often for splicing of theoretically identical fibers we obtain $|A_{12}^{(-)}|_{1310\text{nm}} > |A_{12}^{(-)}|_{1550\text{nm}}$ and $A_{21}^{(+)}|_{1310\text{nm}} > A_{21}^{(+)}|_{1550\text{nm}}$ (1310 nm, 1550 nm denote measurement wavelength), though they do not differ significantly and $A_S \approx 0$ (see Fig. 4) here the splice No. 3 does not comply with the norm, and this is an example of a big noncentricity of the connection.

Case I.2. – $W_1 \neq W_2$, $d = 0$ and when $W_1 > W_2$ then W_1/W_2 decreases along with the wavelength λ , i.e., $(W_1/W_2)|_{1310\text{nm}} > (W_1/W_2)|_{1550\text{nm}}$.

It is a case of splicing of fibers DS SMF and NZDS SMF with the fibers SMF – Fig. 2. Taking into consideration (20), (21) and (22), (23) for splicing of the above mentioned fibers, we receive: $|A_{12}^{(-)}|_{1310\text{nm}} > |A_{12}^{(-)}|_{1550\text{nm}}$ and $A_{21}^{(+)}|_{1310\text{nm}} > A_{21}^{(+)}|_{1550\text{nm}}$. Values $|A_{12}^{(-)}|$ and $A_{21}^{(+)}$ are big $A_S \gg 0$ and $A_S|_{1310\text{nm}} > A_S|_{1550\text{nm}}$. In Figure 5 the experimental confirmation of the above presented analysis has been presented.

Case I.3. – $W_1 \neq W_2, d=0$ and when $W_1 > W_2$ then W_1/W_2 rises along with the wavelength λ , i.e., $(W_1/W_2)|_{1310\text{nm}} < (W_1/W_2)|_{1550\text{nm}}$.

This is the case of splicing of fibers DC SMF with MC SMF. Fibers used in telecommunications DC SMF and MC SMF do not differ much in respect of their mode field diameters [10]. Taking into consideration (20), (21) and (22), (23) for splicing of the above fibers, we obtain $|A_{12}^{(-)}|_{1310\text{nm}} < |A_{12}^{(-)}|_{1550\text{nm}}$ and $A_{21}^{(+)}|_{1310\text{nm}} < A_{21}^{(+)}|_{1550\text{nm}}$, A_S is not big (small differences W_1 and W_2) and actually does not decrease along with both the time and splicing currents increase – Fig. 6 (no influence of optimization), and $A_S|_{1310\text{nm}} < A_S|_{1550\text{nm}}$ which is very characteristic. In Figures 6 and 7 the experimental confirmation of the above presented analysis has been shown.

Case I.4. – $W_1 \neq W_2, d=0$ and $W_1 > W_2$ and $(W_1/W_2)|_{1310\text{nm}} = (W_1/W_2)|_{1550\text{nm}}$.

This is the case of splicing fibers of the same type but differing with mode field radii within the accepted value of MDF (mode field diameter) distribution, e.g., splices MS SMF-MC SMF with $2W_1|_{1310\text{nm}} = 9.0 \mu\text{m}$ and $2W_1|_{1550\text{nm}} = 9.3 \mu\text{m}$.

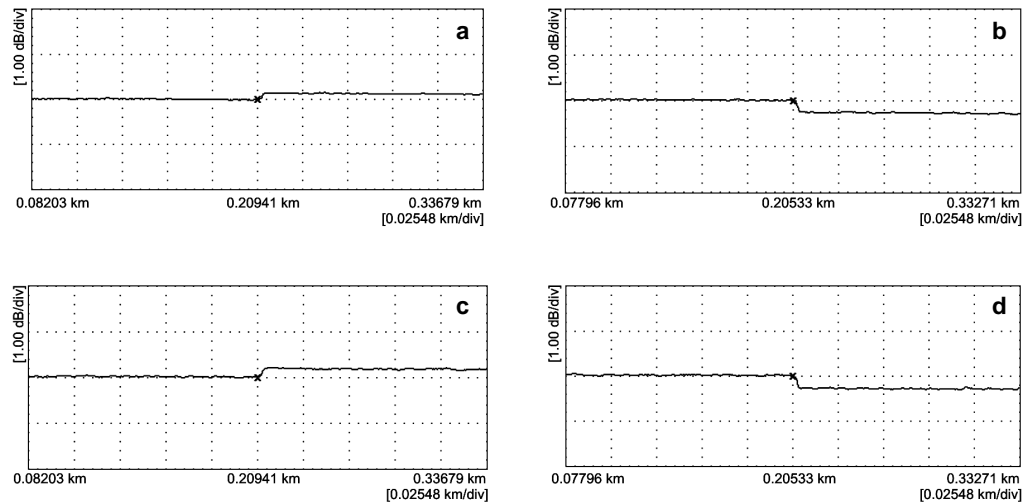


Fig. 6. Reflectometric measurement (reflectometer Anritsu MW9070B was used) of fiber splice MC SMF ($2W_1|_{1310\text{nm}} = 9.3 \pm 0.5 \mu\text{m}$, $2W_1|_{1550\text{nm}} = 10.5 \pm 1 \mu\text{m}$) and DC SMF ($2W_2|_{1310\text{nm}} = 8.8 \pm 0.7 \mu\text{m}$, $2W_2|_{1550\text{nm}} \approx 9.8 \pm 1 \mu\text{m}$): $A_{12}|_{1310\text{nm}}$ (a), $A_{21}|_{1310\text{nm}}$ (b), $A_{12}|_{1550\text{nm}}$ (c), $A_{21}|_{1550\text{nm}}$ (d). Ericsson splicer 925 RTC was used: splicing current $I = 17 \text{ mA}$, splicing time $t = 3.5 \text{ sec}$.

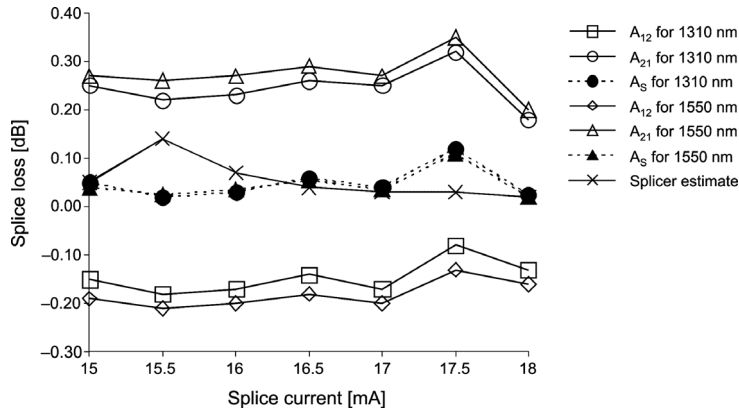


Fig. 7. Dependence of the loss (reflectometric measurement) of fiber splices MC SMF ($2W_1|_{1310\text{nm}} = 9.3 \pm 0.5 \mu\text{m}$, $2W_1|_{1550\text{nm}} = 10.5 \pm 1 \mu\text{m}$) and DC SMF ($2W_2|_{1310\text{nm}} = 8.8 \pm 0.7 \mu\text{m}$, $2W_2|_{1550\text{nm}} \approx 9.8 \pm 1 \mu\text{m}$) on the splicing current – Ericsson splicer 925 RTC, splicing time $t = 3.5$ sec. Reflectometer MW90700B of Anritsu firm was used.

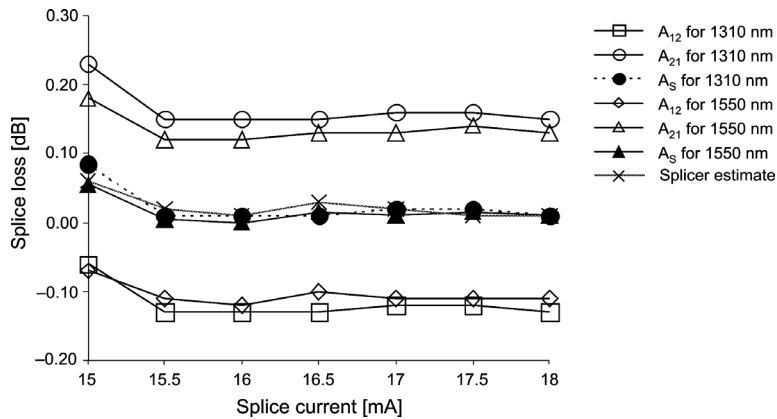


Fig. 8. Dependence of the loss (reflectometric measurement) of fiber splices MC SMF-MC SMF ($2W_1|_{1310\text{nm}} = 9.3 \pm 0.5 \mu\text{m}$, $2W_1|_{1550\text{nm}} = 10.5 \pm 1 \mu\text{m}$) on the splicing current – Ericsson splicer 925 RTC, splicing time $t = 3$ sec. Reflectometer MW90700B of Anritsu firm was used.

Taking into consideration (20), (21) and (22), (23) for splices of the above mentioned fibers, we receive: $|A_{12}^{(-)}|_{1310\text{nm}} = |A_{12}^{(-)}|_{1550\text{nm}}$, $A_{21}^{(+)}|_{1310\text{nm}} = A_{21}^{(+)}|_{1550\text{nm}}$ and $A_S|_{1310\text{nm}} = A_S|_{1550\text{nm}}$ – in practice for this type of splices $A_S|_{1310\text{nm}} > A_S|_{1550\text{nm}}$ – see Fig. 8.

For the applied changes of the current of splicing – Figs. 5–8 the deterioration of quality of splices is not noticed [11].

3.2.2. Noncentral splicing $d \neq 0$

Case II.1. – $W_1 = W_2$, $d \neq 0$. In the expressions (17) and (18) we neglect the first component (insignificant influence):

$$A_{12} = 10 \log \frac{W_2}{W_1} + 20 \log \left[\frac{1}{2} \left(\frac{W_1}{W_2} + \frac{W_2}{W_1} \right) \right] + 4.34 \left(\frac{d^2}{W_1^2 + W_2^2} \right), \quad (24)$$

$$A_{21} = 10 \log \frac{W_1}{W_2} + 20 \log \left[\frac{1}{2} \left(\frac{W_1}{W_2} + \frac{W_2}{W_1} \right) \right] + 4.34 \left(\frac{d^2}{W_1^2 + W_2^2} \right), \quad (25)$$

and we receive:

$$A_{12}|_{1310\text{nm}} = A_{21}|_{1310\text{nm}} = A_s|_{1310\text{nm}} = 4.34 \left(\frac{d^2}{W_1^2 + W_2^2} \right), \quad (26)$$

$$A_{12}|_{1550\text{nm}} = A_{21}|_{1550\text{nm}} = A_s|_{1550\text{nm}} = 4.34 \left(\frac{d^2}{W_1^2 + W_2^2} \right). \quad (27)$$

Equations (26) and (27) obviously are always positive.

Because the mode field rises along with the wavelength $A_s|_{1310\text{nm}} > A_s|_{1550\text{nm}}$. Thus, if one-way reflectometric measurements are always positive and $A_s|_{1310\text{nm}} > A_s|_{1550\text{nm}}$ it means splicing of fibers of the same type in which occurs the fiber axis shift. An example of such a splice is the splice No. 3 in Fig. 4. Having mode field diameters, we can calculate the shift d .

Case II.2. – $W_1 \neq W_2$, $d \neq 0$, and when $W_1 > W_2$ then W_1/W_2 decreases with the wavelength λ , i.e., $(W_1/W_2)|_{1310\text{nm}} > (W_1/W_2)|_{1550\text{nm}}$.

This is the case of splicing of fibers DS SMF and NZDS SMF with fibers MC SMF and DC SMF – Fig. 3, with a simultaneous occurrence of the spliced fibers shift. These fibers significantly differ in mode field diameters. One-way losses $|A_{12}^{(-)}|$ and $A_{12}^{(+)}$ in splices of such fibers achieve values above 1 dB, whereas the axis shift $d = 1 \mu\text{m}$ during splicing of such fibers causes a relatively small loss: of the order 0.07 dB for $\lambda = 1310 \text{ nm}$, and 0.05 dB for $\lambda = 1550 \text{ nm}$.

As a result of analysis of Eqs. (24) and (25) we receive: $|A_{12}^{(-)}|_{1310\text{nm}} > |A_{12}^{(-)}|_{1550\text{nm}}$ for small axis shifts d and $A_{21}^{(+)}|_{1310\text{nm}} > A_{21}^{(+)}|_{1550\text{nm}}$. Values $|A_{12}^{(-)}|$ and $A_{21}^{(+)}$ are big, $A_s \gg 0$ and $A_s|_{1310\text{nm}} > A_s|_{1550\text{nm}}$.

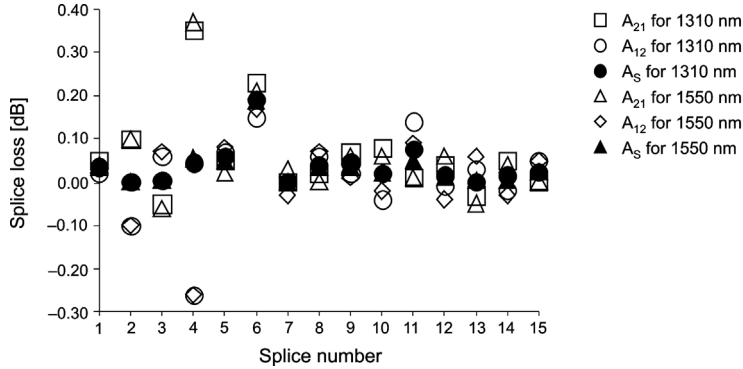


Fig. 9. Loss of 15 splices of joined fibers DC SMF–MC SMF (examples from the used fiber track) for $\lambda = 1310$ nm and $\lambda = 1550$ nm. Reflectometer MW90700B by Anritsu firm was used.

In practice if the shift is not very big $d \leq 1 \mu\text{m}$ the cases I.2 and II.2 cannot be distinguished.

Case II.3. – $W_1 \neq W_2$, $d \neq 0$ and when $W_1 > W_2$ then W_1/W_2 grows with the wavelength λ , e.g., $(W_1/W_2)|_{1310\text{nm}} < (W_1/W_2)|_{1550\text{nm}}$.

This is the case of splicing of fibers DC SMF with fibers MC SMF when a shift of spliced axes occurs. Mode field diameters of fibres used in telecommunications DC SMF and MC SMF do not differ much. One-way losses $|A_{12}^{(-)}|$ and $A_{12}^{(+)}$ of splices of such fibers reach values equal to 0.10–0.15 dB, whereas the axis shift $d = 1 \mu\text{m}$ for splicing of these fibers introduces a relatively big loss: equal to 0.07 dB for $\lambda = 1310$ nm, and to 0.05 dB for $\lambda = 1550$ nm.

The analysis of Eqs. (24) and (25) leads to only one univocal conclusion: thus, if $A_{21}^{(+)}$ is big and A_{12} approaches zero or assumes positive values a big axis shift occurs d (e.g., splice No. 6 in Fig. 9) which can be calculated basing on one-way measurements $A_{12}|_{1310\text{nm}}$ and $A_{12}|_{1550\text{nm}}$.

Case II.4. – $W_1 \neq W_2$, $d \neq 0$, $W_1 > W_2$ and $(W_1/W_2)|_{1310\text{nm}} = (W_1/W_2)|_{1550\text{nm}}$.

This is the case of splicing fibers of the same types but differing with mode field radii distribution MDF (mode field diameter) within the accepted value, e.g., splices MC SMF–MC SMF with $2W_1|_{1310\text{nm}} = 9.0 \mu\text{m}$ and $2W_1|_{1550\text{nm}} = 9.3 \mu\text{m}$ with simultaneous occurrence of the spliced fibers axes shift.

As a result of the analysis of Eqs. (24) and (25) we receive: $|A_{12}|_{1310\text{nm}} < |A_{12}|_{1550\text{nm}}$ and $A_{21}^{(+)}|_{1310\text{nm}} > A_{21}^{(+)}|_{1550\text{nm}}$. In consequence $A_s|_{1310\text{nm}} > A_s|_{1550\text{nm}}$. Having at disposal one-way measurements $A_{12}|_{1310\text{nm}}$ and $A_{12}|_{1550\text{nm}}$ the axis shift d can be calculated.

4. Influence of splicing optimization on reflectometric one-way and two-way splices loss of fibers with significantly different mode field diameters

Fibers NZDS SMF of the type TrueWave and MC SMF 1528 with parameters given in Tab. 1 have been used for the tests. Furukaw's splicer, S-199, was applied. The splicing process was optimized with changing time of splicing without changing the current of the main splicing. Splicing parameters have been presented in Tab. 2.

Table 1. Parameters of spliced fibers [10].

	Refraction coefficient profile	$2W_{1310}$ [μm]	$2W_{1550}$ [μm]	Manufacture technology
MC SMF		9.2 ± 0.4	10.5 ± 1	OVD
NZDS SMF		6.62 [13]	8.4 ± 0.6	MCVD

Table 2. Numbers and parameters of splicing programs.

No.	1	2	3	4	5	6	7	8	9	10	11
Time [ms]	750	1750	3000	5000	8000	12000	15000	18000	20000	25000	30000
Current [rel. u.]	70	70	70	70	70	70	70	70	70	70	70

Optimization of splicing procedures for fibers with significantly different parameters involves increasing splicing current or time, or both parameters simultaneously [12], in relation to currents and times of splicing the standard fibers SMF. The aim of increasing splicing time and current is diffusion of the core dopant in the spliced fibers so as to equalize the diameters of mode fields $2W_1$ and $2W_2$ within the splice [13]. Increasing only the splicing time is, however, safer as increasing the current causes a fast temperature rise and can lead to melting instead of splicing of the fibers.

5. Analysis of reflectometric measurements of optimized fiber splices with significantly different mode field diameters – method of evaluation of process optimization

In Figures 10 and 11 the measurement results of one-way loss A_{21} and A_{12} of fibers NZDF SMF–MC SMF splices as a function of splicing time have been presented.

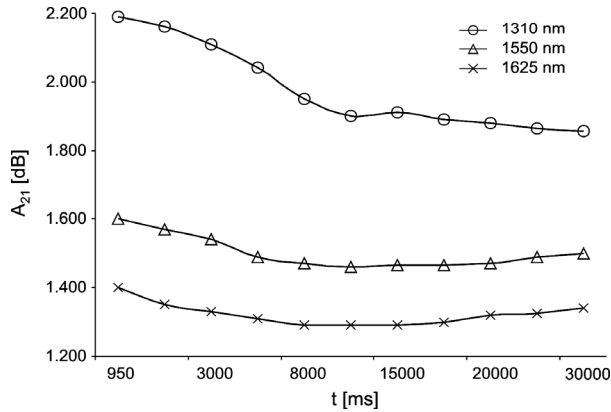


Fig. 10. Dependence of one-way loss A_{21} (for three measurement wavelengths) of fiber NZDS SMF-MC SMF splices on the splicing time.

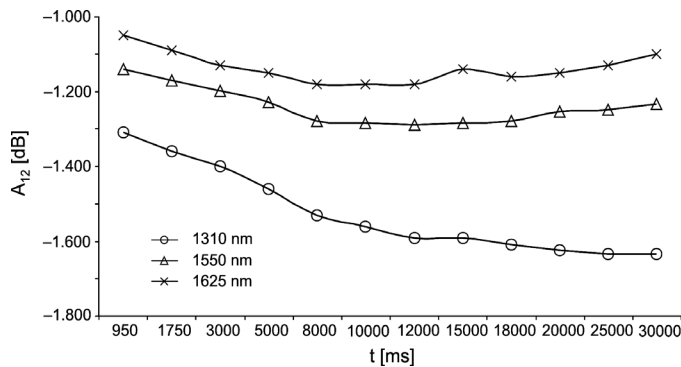


Fig. 11. Dependence of one-way loss A_{12} (for three measurement wavelengths) of fiber NZDS SMF-MC SMF splices on the splicing time.

In Fig. 12 true loss A_S has been shown for the same splicing times. The presented results are the average of at least 10 splicing tests for each point. The measurements were made with the use of reflectometer MW9076D\D1 produced by Anritsu firm for three measurement lengths $\lambda = 1310$ nm, $\lambda = 1550$ nm, $\lambda = 1625$ nm. Measurements for three wavelengths (Figs. 10–12) confirm the theoretical analysis, *i.e.*, loss decrease A_{21} , A_{12} and A_S along with the wave length increase for this type of fibers.

True loss of splices A_S decreases with the increase of the splicing time – Fig. 12. We may assume that the mode fields of spliced fibers match (19) because of the dopant diffusion – Fig. 13. However, the author's and others' research [14] concerning localization of the transient area, with the use of Roentgen microanalysis methods within the splice, Fig. 13, did not prove explicitly the existence of such an area. An unquestionable evidence that in the optimization process, with increasing time and splicing current, the mode field diameters matching $2W_1 \leftrightarrow 2W_2$ occurs, is the reproducibility of one-way loss A_{21} and A_{12} as a function of splicing time – Figs. 10, 11.

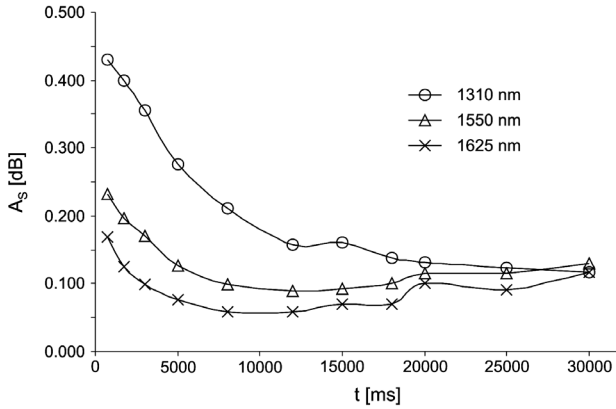


Fig. 12. Dependence of true loss A_s (for three measurement wavelengths) of fiber NZDS SMF–MC SMF splices on the splicing time.

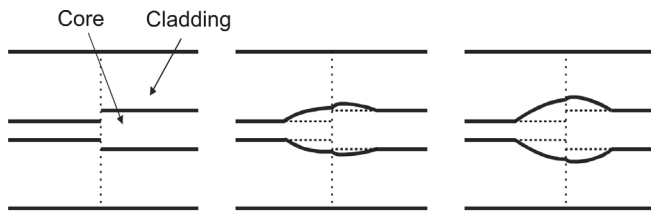


Fig. 13. Rising of a transient area.

Thus, we can notice that $A_{21}^{(+)}$ decreases and $A_{12}^{(-)}$ increases along with the splicing time (Figs. 10, 11) and splicing current (Fig. 5). The A_{12} and A_{21} are described by the expressions (17) and (18). In these expressions components: $[10\log(n_2/n_1) + 10\log(W_2/W_1)]$ for A_{12} and $[10\log(n_1/n_2) + 10\log(W_1/W_2)]$ for A_{21} result from a measurement method, *i.e.*, backscattered (15), and are not subject to optimization as they depend on backscattered power in the fibers used for splicing.

“Optimization” affects only components resulting from optical power coupling

between the spliced fibers, *i.e.*, $20 \log \left[\frac{1}{2} \left(\frac{W_1}{W_2} + \frac{W_2}{W_1} \right) \right]$ or $20 \log \left[\frac{1}{2} \left(\frac{W_1}{W_2} + \frac{W_2}{W_1} \right) \right] + 4.34 \left(\frac{d^2}{W_1^2 + W_2^2} \right)$ in case of the axis shift, both for A_{12} and for A_{21} . Thus, if as in

Fig. 11, $|A_{12}^{(-)}|$ rises which means that because $10 \log \frac{n_2}{n_1} + 10 \log \frac{W_2}{W_1}$ remains

constant negative, the always positive $20 \log \left[\frac{1}{2} \left(\frac{W_1}{W_2} + \frac{W_2}{W_1} \right) \right]$, or $20 \log \left[\frac{1}{2} \left(\frac{W_1}{W_2} + \frac{W_2}{W_1} \right) \right] + 4.34 \left(\frac{d^2}{W_1^2 + W_2^2} \right)$, in case of axis shift, must decrease.

This in turn means that W_1/W_2 approaches one – so the mode fields matching occurs.

As a result of the core dopant diffusion W_1 approaches W_2 , but at the same time the

mode field radii within the splice increase – Fig. 13. This fact causes that

$4.34 \left(\frac{d^2}{W_1^2 + W_2^2} \right)$ decreases as well (if there is a shift of the spliced fibers axis).

At the same time the positive $A_{21}^{(+)}$ (Fig. 10) decreases and because

$10 \log \frac{n_1}{n_2} + 10 \log \frac{W_1}{W_2}$ remains positive constant, the $20 \log \left[\frac{1}{2} \left(\frac{W_1}{W_2} + \frac{W_2}{W_1} \right) \right]$, or

$20 \log \left[\frac{1}{2} \left(\frac{W_1}{W_2} + \frac{W_2}{W_1} \right) \right] + 4.34 \left(\frac{d^2}{W_1^2 + W_2^2} \right)$ when the axes of spliced fibers are

shifted, must always decrease. This means that W_1/W_2 approaches one—there occurs mode fields matching.

The increase in splices loss when the splicing time is exceeded by about 20000 milliseconds for $\lambda = 1550$ nm and $\lambda = 1625$ nm, with a constant decrease loss for $\lambda = 1310$ nm (Fig. 12) is most probably connected with nonhomogeneities which occur in the cladding during very long splicing time. Along with increasing λ the mode field grows, and therefore, nonhomogeneities in the cladding cause the increase of splicing loss for larger measurement wavelengths. It is also the splice quality evaluation index and a signal to stop increasing splicing time or current.

6. Conclusions

On the basis of reflectometric, one-way measurements of splice damping the types of spliced fibers can be identified. It is important because most frequently while measuring the so-called route we do not possess information what types of fibers are included in this route. Other measurements, for instance transmission ones, do not provide such possibilities.

Optimized spliced fiber joints with significantly different parameters are characterized by large negative $A_{12}^{(-)}$ and positive $A_{21}^{(+)}$ one-way losses and at the same time by a small, meeting the requirements, true loss A_S . Norms and recommendations, e.g. [15], concerning small values of one-way losses of spliced joints can only warn of connecting fibers of different types, but they cannot decide about true loss and the quality of splices.

Optimization process of fibers with significantly different parameters can be verified by one-way reflectometric splice loss measurements. Analysis of these measurements, especially for an extended range of measurement wavelengths, allows

to define explicitly if there occurs mode fields matching process of the spliced fibers, and when to stop the optimization process, as there occurs the degradation of the splice.

References

- [1] SNYDER A.W., *Optical Waveguide Theory*, Chapman and Hall, London 1983.
- [2] HEWLETT S.J., LADOUCEUR F., LOVE J.D., *Splice loss in single- and twin-core buried channel waveguide devices*, *Optical and Quantum Electronics* **26**(1), 1994, pp. 45–62.
- [3] GALLAWA R.L., KUMAR A., WEISSHAAR A., *Fibre splice loss: a simple method of calculation*, *Optical and Quantum Electronics* **26**(3), 1994, pp. S165–72.
- [4] MAJEWSKI A., *Teoria i projektowanie światłowodów*, WNT, Warszawa 1991 (in Polish).
- [5] NEUMANN E.G., *Single-Mode Fibers*, Springer-Verlag 1988.
- [6] NAKAZAWA M., *Rayleigh backscattering theory for single-mode optical fibers*, *Journal of the Optical Society of America* **73**(9), 1983, pp. 1175–80.
- [7] SZUSTAKOWSKI M., *Elementy Techniki Światłowodowej*, WNT, Warszawa 1992 (in Polish).
- [8] MILLER C.M., METTER S.C., WHITE I.A., *Optical Fiber Splices and Connectors*, Marcel Dekker Inc., New York and Basel 1986.
- [9] KAISER G., *Optical Fiber Communications*, McGraw Hill, New York 2001.
- [10] BARBIERI A., *A Guide to Select Single – Mode Fibers for Optical Applications*, Cisco Systems 2001.
- [11] RATUSZEK M., MAJEWSKI J., ZAKRZEWSKI Z., STRÓŻECKI S., ZALEWSKI J., *Arc fusion splicing of telecommunication optical fibers in extreme climatic circumstances*, *Proceedings of the SPIE* **4239**, 2000, pp. 150–4.
- [12] RATUSZEK M., MAJEWSKI J., ZAKRZEWSKI Z., ZALEWSKI J., *Examination of spliced telecommunication fibers of the NZDS-SMF type adjusted to wavelength division multiplexing*, *Optica Applicata* **29**(1-2), 1999, pp. 73–85.
- [13] RATUSZEK M., MAJEWSKI J., ZAKRZEWSKI Z., RATUSZEK M.J., *Process optimisation of the arc fusion splicing different types of single mode telecommunication fibres*, *Opto-Electronics Review* **8**(2), 2000, pp. 161–70.
- [14] HEJNA J., RATUSZEK M., MAJEWSKI J., ZAKRZEWSKI Z., *Scanning electron microscopy examination of telecommunication single mode fiber splices*, *Optica Applicata* **33**(4), 2003, pp. 583–9.
- [15] Norm of TP S.A. Poland: ZN -96/TP S.A. - 002/T.

*Received July 26, 2004
in revised form December 17, 2004*